



Analysis of long range dependence in the EEG signals of Alzheimer patients

T. Nimmy John¹ · Subha D. Puthankattil¹ · Ramshekhar Menon²

Received: 16 June 2017 / Revised: 14 November 2017 / Accepted: 19 December 2017 / Published online: 5 January 2018
© Springer Science+Business Media B.V., part of Springer Nature 2018

Abstract

Alzheimer's disease (AD), a cognitive disability is analysed using a long range dependence parameter, hurst exponent (HE), calculated based on the time domain analysis of the measured electrical activity of brain. The electroencephalogram (EEG) signals of controls and mild cognitive impairment (MCI)-AD patients are evaluated under normal resting and mental arithmetic conditions. Simultaneous low pass filtering and total variation denoising algorithm is employed for preprocessing. Larger values of HE observed in the right hemisphere of the brain for AD patients indicated a decrease in irregularity of the EEG signal under cognitive task conditions. Correlations between HE and the neuropsychological indices are analysed using bivariate correlation analysis. The observed reduction in the values of Auto mutual information and cross mutual information in the local antero-frontal and distant regions in the brain hemisphere indicates the loss of information transmission in MCI-AD patients.

Keywords Alzheimer's disease · EEG · Multi-resolution decomposition · Hurst exponent · Auto mutual information · Cross mutual information

Introduction

Dementia is a progressive mental disorder which affects the working memory of a person. It is widely known that the reduction of motor functions and thought processes are the characteristics of dementia of which Alzheimer's is the most prominent. The accumulation of plaques and tangles in the brain cells are considered to be the main cause of Alzheimer's. Alzheimer's is not a normal part of aging. Alzheimer's Statistics 2015 reported that 44 million people suffer from Alzheimer's or dementia. Alzheimer's disease international (ADI) stated that, in India, the number of people suffering from dementia are expected to rise 12 million by 2050. Alzheimer's Association 2016 informed

that 15–20% of people above the age of 65 have mild cognitive impairment.

Changes in behavior, language and learning problems are observed in demented people (Letemendia and Pampiglione 1958). Analysis of electroencephalogram (EEG), a measure of the electrical functioning of brain, could lead to the development of an indicator of Alzheimer's disease, presenile dementia, Pick's disease, Jakob-Creutzfeldt's disease etc. EEG, being a noninvasive study, is used for the extraction of features to characterize the disease. Absence of alpha rhythm, highest four point scale mean score, large dementia differentials and slowing of EEG could separate Alzheimer Disease from other diseases (Gordon and Sim 1967). Memory impairment, formation of senile plaques and neurofibrillary tangles, reduction of acetylcholinesterase and choline acetyltransferase etc. are some of the changes observed in the brain of Alzheimer subjects. National Institute of Neurological and Communicative Disorders and Stroke-Alzheimer's Disease and Related Disorders Association (NINCDS-ADRDA) has developed a criterion for identifying Alzheimer's (McKhann et al. 1984). Reduction of mobility (Loechesa et al. 1991), lower dipolarity (Hara et al. 1999), sensitive directional

✉ Subha D. Puthankattil
subhadp@nitc.ac.in

¹ Department of Electrical Engineering, National Institute of Technology Calicut, Kozhikode, India

² Department of Neurology, Sree Chitra Tirunal Institute for Medical Sciences and Technology, Thiruvananthapuram, India

information flux (Babiloni et al. 2009) and diminished clustering coefficient and path length (Stam et al. 2009) are used for distinguishing AD from normal controls. EEG slowing is noted in AD especially on temporal, parieto-occipital, and frontal regions (Petit et al. 1993). Compared with normal, EEG abnormalities are recognized in the progression of Alzheimer's disease. Large amount of neuronal loss is verified in some of the AD patients (Rae et al. 1987).

Quantitative Electroencephalography (QEEG) frequency analysis has been reported to be useful for dementia diagnosis (Nuwer 1997). Impairment of high to low EEG frequency ratio is observed in the left temporal region of demented patients (Grunwald et al. 2002; Leuchter et al. 1987). A rise in delta-theta values and a reduction of mean frequency and alpha-beta values has been identified in Alzheimer EEG (Coben et al. 1990; Fonseca et al. 2011). The slowing of alpha frequency band is the hallmark of EEG in Alzheimer's disease (Bhattacharya et al. 2013). Increased values of mean frequency ratio are observed in AD patients (Stigsby et al. 1981). A reduced mean dominant occipital frequency is detected in AD than in healthy controls (Prinz and Vitiell 1989; Pucci et al. 1999). Vanishing of 40 Hz frequency is recognised in AD patient at the problem solving task (Raghavan et al. 1986).

Visual and spectral EEG analysis help in differentiating AD with mild cognitive impairment (Brenner et al. 1988; Waser et al. 2013). Power spectrum analysis and topographic EEG mapping have revealed the decelerating of background EEG (Buchan et al. 1997). The power spectrum of Alzheimer's showed the absence of dominant action in the 6.5–12 Hz band. Increased power in 1–6.5 Hz band is also observed in AD (Davide et al. 2004; Fonseca et al. 2011; Gasser et al. 1994; Klimesch 1999; Pucci et al. 1998; Wada et al. 1997; Wang et al. 2015). A decrease in the relative logarithmic transformed power spectral density has been reported in the right temporal of AD patients (Aghajani et al. 2013). The paraconsistent artificial neural network (PANN) was capable of accurately recognizing slowing of alpha rhythm in Alzheimer patient (Abe et al. 2007).

The reduction of coherence in AD indicates a decline in cortical connectivity (Sankari et al. 2011). Reduced inter-hemispheric theta coherence and left temporal alpha coherence were observed in AD patients (Adler et al. 2003; Anghinah et al. 2011; Fonseca et al. 2013, 2015; Kikuchi et al. 2002). AD subjects had a diminished upper alpha coherence between right temporal and central cortex (Hogan et al. 2003) and have used multiple regression models to assure this conclusion (Brunovsky et al. 2003). Damage of cortico-cortical or cortico-subcortical networks in AD revealed a reduction of alpha coherence in temporal-parieto-occipital regions (Locatelli et al. 1998). Decreased

wavelet coherence is observed in Alzheimer's in comparison with healthy controls (Jeong et al. 2016). The relative power spectral density (PSD) estimated using AR Burg method and coherence of EEG signals from AD patients are evaluated in order to detect the abnormalities displayed in the response from cortico-cortical region (Wang et al. 2015).

Synchrony measures show decreased EEG synchrony in MCI patients (Dauwels et al. 2010). EEG synchrony markers have been correlated with Mini-Mental State Examination (MMSE) that measures the severity of AD (Waser et al. 2016). A decrease of beta and lower alpha synchronization is observed in multi-channel EEG of mild AD patients (Pijnenburg et al. 2004; Stam et al. 2005). Progressively decreased delta and alpha synchronization likelihood is identified in MCI and mild AD groups (Babiloni et al. 2006; Duffy et al. 1984). The global field synchronization (GFS) is found to be lower in AD than in normal (Koenig et al. 2005; Park et al. 2008). Lower values of synchronization likelihood and improved Omega complexity are observed in AD patients at the 0.5–25 Hz frequency ranges (Czigler et al. 2008).

AD patients have been characterized with lower Lyapunov exponent (L1) and correlation dimension (D2) (Carlino et al. 2012; Jeong and Kim 1997; Jeong et al. 1998). A lower Approximate Entropy (ApEn) in the AD subjects at P3 and P4 electrodes shows the decline of irregularity in Alzheimer patients (Abasolo et al. 2005). A decrease in the Lempel–Ziv (LZ) complexity and multiscale Lempel–Ziv complexity of EEG patterns are observed in AD subjects (Abasolo et al. 2006; Liu et al. 2016). Lower irregularity is found in AD patients in the calculation of spectral entropy than healthy controls (Hornero et al. 2008). Global coherence and global correlation dimension (D2) having changes in the higher frequency ranges indicate decreased cortical functional connectivity (Carlino et al. 2012; Jelles et al. 2008). Higher order spectra (HOS) and quadratic phase coupling of spontaneous human speech signals are analysed for the early diagnosis of AD (Nasrolahzadeh et al. 2016). The combinations of relative PSD and multiscale LZC are used as input feature for the classification of two groups (Liu et al. 2016). Dynamical stationarity of EEG at the frontal and temporal regions of the brain distinguishes AD patients from normal controls (Vincent et al. 2008). Nonlinear analysis of EEG and magnetoencephalogram (MEG) of AD patients revealed less complexity and more regularity of the signals than that of the healthy controls (Hornero et al. 2009). Both slowing and loss of complexity of EEG is found in MCI and Mild AD than normal group (Dauwels et al. 2011; Wan et al. 2008). Quantification of Multiscale entropy (MSE) complexity in EEG signals is used for assessing the cognitive and neuropsychiatric severity of

AD (Escudero et al. 2006; Mizuno et al. 2010; Tsai et al. 2012; Yang et al. 2013). The reduction of compression ratio and entropic measures are considered as the hallmark of onset of AD (Morabito et al. 2013). Multivariate multiscale entropic complexity measures of Alzheimer's disease showed better results than single scale analysis (Labate et al. 2013). Reduced fractal dimension is reported in Alzheimer group than normal subjects (Besthorn et al. 1995; Smits et al. 2016; Woyshville and Calabrese 1994). Multivariate Multi-Scale Permutation Entropy is used for analyzing the complexity of AD EEG signals (Morabito et al. 2012). Entropy and auto mutual information describes the complexity of AD EEG signal with MMSE scores (Coronel et al. 2017). Multivariate and univariate multiscale complexity analysis have been used for the characterization of complexity of EEG frequency bands of AD (Azami et al. 2017). The combinations of nonlinear and linear features provided better class separability (Balli and Palaniappan 2010). The resting-state EEG dynamics of the early stage of Parkinson's disease (PD) revealed lower permutation entropy (PE) and higher order index (OI) for patients than controls (Yi et al. 2017). Nonlinear measures extracted from EEG signals under emotional processing of PD patients with respect to motor symptom asymmetry, suggests deficiency of emotional communication in patients with right hemisphere dysfunction (Yuvaraj and Murugappan 2016). Hurst Exponent (HE) can be used for the detection of epileptic seizure (Osorio and Mark 2007). The HE values exhibited long range anti-correlation in both epileptic and interictal EEG (Geng et al. 2011). Combined nonlinear features of sample entropy with detrended fluctuation analysis (DFA) and kolmogorov complexity are used to evaluate functional plasticity changes in spontaneous EEG recordings of rats before and after spinal cord injury (SCI) (Pu et al. 2016).

Prominent changes in temporal regions are noted in AD patients than that of normal controls (Breslau et al. 1989). Functional disconnection (Tóth et al. 2014), reduced corpus callosum cross-sectional area (Pogarell et al. 2005) and decreased Relative Wavelet Energy (RWE) (Jeong et al. 2016) helps to identify AD. Statistical pattern recognition (Snaedal et al. 2010, 2012), Automatic recognition (Kim et al. 2005), Machine learning approach (Podgorelec 2012), Discrete wavelet transform (DWT) (Ghorbanian et al. 2013), Continuous wavelet transform (CWT) (Ghorbanian et al. 2015) are some of the techniques used for AD analysis.

Magnetic resonance imaging (MRI) and functional MRI are the brain imaging techniques that has been used in studies for the diagnosis of AD. Scale-invariant feature transforms (SIFT) are used for extracting the features from the different slices of MRI images, which are then ranked using Fisher's discriminant ratio. The use of Support vector

machines with different kernels provide a classification accuracy of 86% in classifying the MR images of mild AD patients from healthy controls using the histogram developed from SIFT features (Daliri 2012). Low frequency fluctuations (LFF) connectivity analysed using resting state Functional MRI studies (fMRI) revealed highly disturbed functional connectivity between different regions of the brain in early AD patients (Wang et al. 2007). Brain activation patterns are observed to be altered in the fMRI images, during the early stages of Alzheimer's than in controls with normal aging. This study involved association encoding task (Sperling et al. 2003). Patterns obtained from MRI images were used for detecting abnormality in the structure of the brain of early stages of MCI-AD patients. These patterns were further used as feature for classification which gave 90% classification accuracy (Davatzikos et al. 2008). Linear support vector machines (SVM) are used for the automated classification of AD patients from normal individuals using the gray matter segment of T1-weighted structural MRI scans (Kloppel et al. 2008). Structural MRI and advanced MRI techniques such as arterial spin labeling (ASL) and diffusion tensor imaging (DTI) are employed for the classification using SVM for differentiating AD, fronto temporal dementia (FTD) and controls (Bron et al. 2017). Proportional odds model were used to assess the rate of atrophy of entorhinal and hippocampal volumes and size to predict the risk of incident AD using MRI images (Stoub et al. 2005). Decreased functional connectivity (FC) was observed for AD patients within the default-mode network (DMN) from the studies conducted using resting state fMRI (rs-fMRI) (Binnewijzend et al. 2012).

The combination of subspace filtering and independent component analysis (ICA) method (Melissant et al. 2005; Vorobyov and Cichocki 2002), blind source separation (BSS) and correlation metrics (Cichocki et al. 2004; Joyce et al. 2004) and Fast ICA or fixed point algorithm of ICA (Mishra and Singla 2013) are used for removing noises in EEG signals.

Studies till date have clearly improved our understanding of AD, its onset, the progress and the consequent influence on the cognitive functions. It also revealed the importance of the development of the signal processing tools for the time series analysis in the characterization of features of Alzheimer's, to be extracted from the EEG signals. The major objective of the present study is to analyze the long range dependence in the EEG time series of MCI-AD patients and healthy controls using Hurst exponent. The loss of information transmission among different regions of the brain is also being evaluated using Mutual Information analysis. The organisation of the paper is explained below: "Materials" section describes an overview of data collection, EEG data recording and

preprocessing used for EEG signal analysis; “[Methods of analysis](#)” section describes the different methods adopted for EEG processing; “[Results](#)” section formulates the results obtained from HE analysis, bivariate analysis and mutual information; followed by a detailed discussion of the paper in the “[Discussion](#)” section part; finally “[Conclusion](#)” section of the paper list out major conclusions of the study

Materials

Data collection

A group control study is adopted for the present analysis. The control group consists of 15 men and 12 women subjects. The cognitive impaired group comprises of 13 subjects which includes six men and seven women. The age group selected for this work ranges from 50 to 80 years including both the sexes. Clinical dementia rating (CDR) (Hughes et al. 1982) scale is used for rating dementia. For the present study we have considered signals with a CDR value ≤ 1 .

EEG data recording

EEG data acquisition from healthy controls and Alzheimer patients are carried out at Sree Chithira Thirunal Institute of Medical Sciences, Trivandrum, Kerala, India. Ethical committee sanction was obtained for this work. Written informed consent is obtained from both controls and subjects who participated in this study. Mini–Mental State Examination (MMSE) (Folstein et al. 1975) is a 30 point test conducted for determining the cognitive impairment. Rey Auditory Verbal Learning Test (RAVLT) (Rosenberg et al. 1984) is assessed for evaluating memory problems. Addenbrooke’s Cognitive Examination (ACE) (Dudas et al. 2005) is evaluated out of 100 and a lower value is an indication of progression of the disease. The mean and standard deviation of the age, MMSE and ACE of the controls and patients participated in this study are shown in Table 1. There is no significant difference in age and education (years) between the two groups as the p value obtained is 0.8979 and $F = 0.02$. But significant differences were observed for patient group and controls for the neuropsychological indices of Mini–Mental State Examination

(MMSE) and Addenbrooke’s Cognitive Examination (ACE) ($F = 20.34$; p value is 0.0001).

The sampling frequency of EEG signal is 400 Hz. A unipolar recording is carried out for data acquisition. Clinical EEG recordings are carried out on a 32-channel digital EEG acquisition system (NicVue, Nicolet-Viking, USA) with the scalp electrodes placed according to the International 10–20 electrode placement system (Jasper 1958). Measurement electrodes are placed at 23 electrode locations: Fp1, Fp2, F3, F4, C3, C4, P3, P4, O1, O2, T1, T2, F7, F8, T3, T4, T5, T6, Fz, Cz, Pz, A1 and A2. The different recording protocols adopted in this work are Eyes Open (EO), Eyes Closed (EC), Mental Arithmetic Eyes Open (MAEO) and Mental Arithmetic Eyes Closed (MAEC) condition. For MAEO and MAEC protocols, simple numerical exercises involving two number addition, subtraction and multiplication was given to the groups (one with keeping their eyes closed [MAEC] and the other with keeping their eyes open [MAEO]). Signal acquisition is carried out for a duration of five minutes each under each recording protocol. Digitized EEG signals are analysed in MATLAB (R2016a) environment.

Figure 1 represents the EEG signal of an Alzheimer patient acquired from T5 location under Eyes Closed condition and Fig. 2 represents the signal from a control acquired from the same location following the same recording protocol.

Preprocessing: removal of noise

Raw EEG always contains artifacts such as Electrocardiogram (ECG), Electromyogram (EMG), power line noises, artifacts due to sweating and respiration. This necessitates the removal of noise for further processing. There exist various noise reduction techniques that include Kalman filtering, ARMA method, ICA, Principle component analysis (PCA), Wavelet denoising etc. Total variation denoising (TVD) is an optimization technique which minimizes the non-differentiable objective function (Rudin et al. 1992). Majorization-minimization (MM) (Condat 2013) and Alternating Direction Method of Multipliers (ADMM) are applied for the low-pass filtering and TVD denoising. Combined LPF/TVD algorithm is used for removing both the high and low frequency noise components from the signal (Selesnick et al. 2014). In this algorithm, the noisy signal is assumed to be consisting of a

Table 1 Mean and standard deviation of Control and Patient

Subject	AGE (years)	MMSE	ACE	Education (years)
Control	56.18 \pm 4.78	29.37 \pm .92	93 \pm 5.34	12.3 \pm 3.5
Patient	67.78 \pm 6.10	23.92 \pm 4.15	63.85 \pm 8.45	11.1 \pm 3.3

Fig. 1 EEG signal of an Alzheimer patient

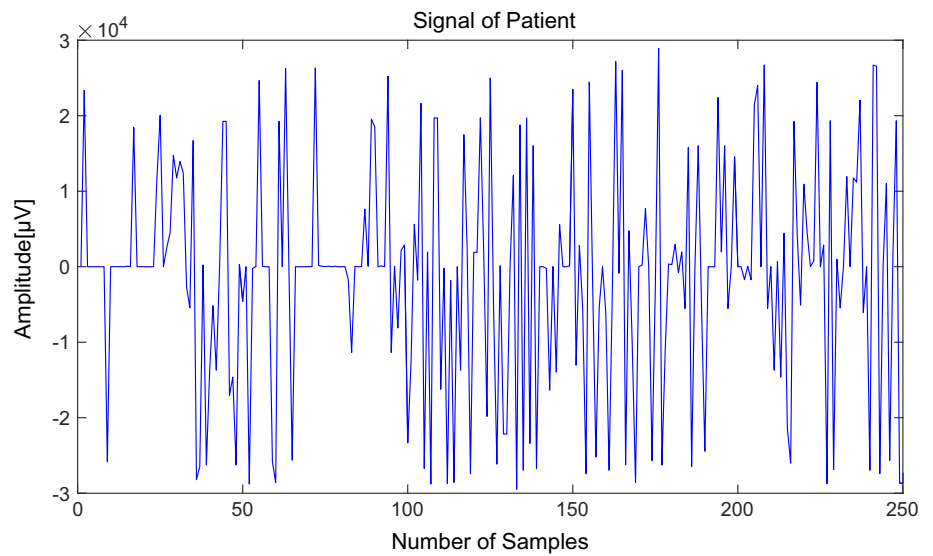
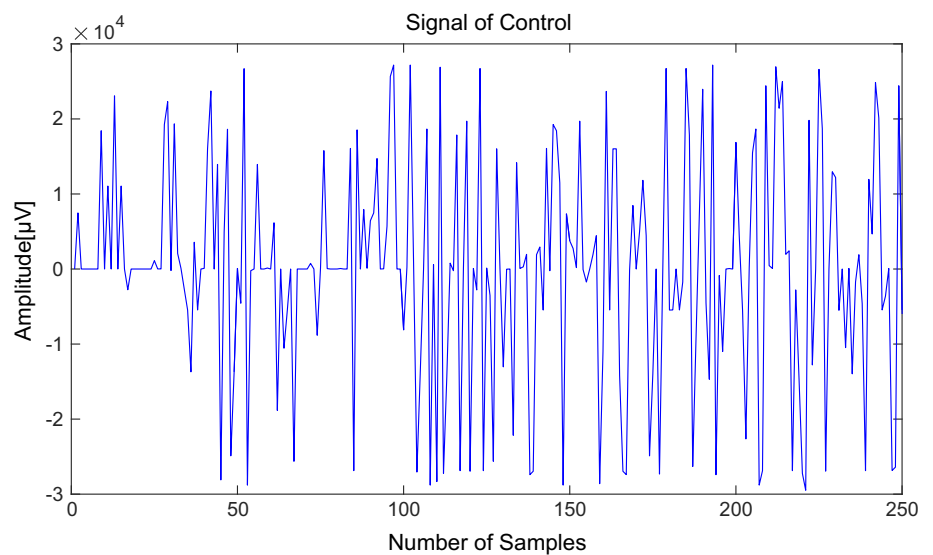


Fig. 2 EEG signal of a control



sparse signal, noise, and low-frequency component. LPF/TVD algorithm works on the sparse data.

Consider a noisy signal y consisting of three components: x - sparse signal, f - low pass component, w - Gaussian noise having variance σ^2 .

$$y = x + w + f \tag{1}$$

Here the estimates of x and f are:

$$f \approx LPF(y - x) \tag{2}$$

Combining (1) and (2)

$$w = (y - x) - LPF(y - x) \tag{3}$$

Hence ‘ w ’ can be rewritten as

$$w = HPF(y - x) \tag{4}$$

$$argmin_x \left\{ \frac{1}{2}(Hy - x_2)^2 + \lambda \|Dx\| \right\} \tag{5}$$

Equation (5) represents the optimization problem. Dx denotes the first order difference. Regularization parameter ‘ λ ’ is used for getting suitable solutions. The high-pass filter H is to be of the form $H = A^{-1}B$, where A and B are banded matrices. Denoising operation is performed assuming values for λ, f_c and d , where f_c is the cut off frequency and d is the filter order parameter. In this work, $f_c = 0.022$, $d = 1$ and $\lambda = 0.1$ are selected based on the optimality condition. The suitability of the values of the parameter can be observed using optimality plot (Selesnick et al. 2014). Validation of noise removal using LPF/TVD algorithm is done by calculating signal to noise ratio (SNR). The enhancement of SNR of the signal proves the efficiency of the denoising algorithm.

Methods of analysis

Multi-resolution decomposition

Multi-resolution signal decomposition is performed using Discrete Wavelet Transform (Mallat 1989). Appropriate Wavelet has to be chosen for the decomposition of the signal. The choice of wavelet is decided by the calculation of correlation coefficient of the signal with the chosen wavelet. db10 is found to have maximum correlation coefficient with more than 95% of the EEG signals acquired in this study. The frequency bands used for the six level decomposition in this study is shown in Table 2. D1 (Detail level 1), D2 (Detail level 2), D3 (Detail level 3), D4 (Detail level 4), D5 (Detail level 6) represent the Detail levels and A6 (Approximation level 6) represents the Approximation level.

Nonlinear parameter: Hurst Exponent (HE)

There exist a number of parameters to assess the nonlinearity of signals. Hurst Exponent (Hurst 1951) is one such parameter which helps in detecting long range dependence of a time series. The present analysis uses rescaled range method (Mandelbrot and Wallis 1969) for calculating HE.

HE is expressed as:

$$HE = \frac{\log\left(\frac{R}{S}\right)}{\log T} \tag{6}$$

where T —duration of the sample of data, $\frac{R}{S}$ —corresponding value of rescaled range.

The algorithm used for evaluating Hurst Exponent is as follows:

Let N - be the total length of the time series, $n = N, N/2, N/4, \dots$

Step 1 Calculation of the mean ‘ m ’

$$m = \frac{1}{n} \sum_{i=1}^n X_i \tag{7}$$

$X_i = X_1, X_2, X_3, \dots$

Step 2 Compute mean-adjusted series ‘ Y_t ’

$$Y_t = X_t - m \quad \text{for } t = 1, 2, \dots, n \tag{8}$$

Step 3 Calculate cumulative deviate series ‘ Z_t ’

$$Z_t = \sum_{i=1}^t Y_i \quad \text{for } t = 1, 2, \dots, n \tag{9}$$

Step 4 Find the range ‘ $R(n)$ ’

$$R(n) = \max(Z_1, Z_2, Z_3, \dots, Z_n) - \min(Z_1, Z_2, Z_3, \dots, Z_n) \tag{10}$$

Step 5 Determine standard deviation ‘ $S(n)$ ’

$$S(n) = \sqrt{\frac{1}{n} \sum_{i=1}^n (X_i - m)^2} \tag{11}$$

Step 6 Compute the rescaled range, ‘ $R(n)/S(n)$ ’

$$H = R(n)/S(n) \tag{12}$$

A long term positive auto correlated time series will have H in the range 0.5 and 1. Uncorrelated data series has an H value of 0.5. Switching of high and low values in the neighboring pairs occur for H in the range of 0–0.5.

Pearson’s correlation coefficient, Spearman’s rank correlation coefficient and Mutual information

Pearson’s correlation coefficient (Product moment correlation) measures dependence between two variables. The value of correlation coefficient lies between -1 and 1. If no correlation exists, then correlation coefficient becomes zero. Spearman’s rank correlation coefficient (Fieller et al. 1957) is the ranked form of Pearson’s correlation. Product moment correlation explains the linear relationship whereas Spearman’s rank correlation describes monotonic relationships. The range of Spearman’s correlation is similar to Pearson’s. EEG very well reflects the information processed in the brain (Jeong et al. 2001). Mutual information (MI) of two variables is the mutual dependence among the variables. MI helps for finding both linear and nonlinear relationship of the series. MI values are always positive. MI gets maximum when the values of the series are exactly same. MI has been used for measuring and analyzing the dynamic coupling between two systems (Cover and Thomas 1991). There exist mainly two types of MI: Auto mutual information (AMI) and Cross mutual information (CMI). AMI explains that the time series values are predicted from the delayed forms of the same series. Cross mutual information describes the dependence of one time series on the other. The studies on MI proves good for estimating the complexity of EEG signals and also

Table 2 Frequency band corresponding to 6-level decomposition

Decomposed signals	Frequency bands (Hz)	Decomposition levels
D1	100–200	1
D2	50–100	2
D3	25–50	3 (Gamma)
D4	12.5–25	4 (Beta)
D5	6.25–12.5	5 (Alpha)
D6	3.125–6.25	6 (Theta)
A6	0–3.125	6 (Delta)

assess the information transmission between various cortical areas of the brain (Abasolo et al. 2008; Jeong et al. 2001). Statistical analysis is conducted by ANOVA for evaluating the significant difference between the groups. Multiple comparisons using Bonferroni correction is applied on the p values obtained.

Results

Multi-resolution Decomposition

A six-level decomposition is carried out on the measured EEG signals using db 10 Wavelet. This particular db 10 was chosen from various wavelets ranging from db2-db10, sym1-sym7 and coif1-coif5 as it gave a higher correlation coefficient with the recorded signals. The six decomposition levels are: D1 (Detail level 1), D2 (Detail level 2), D3 (Detail level 3), D4 (Detail level 4), D5 (Detail level 6) and A6 (Approximation level 6).

Nonlinear parameter: Hurst Exponent (HE)

The nonlinear parameter, Hurst Exponent (HE), is evaluated from the EEG signals recorded from 23 locations of normal controls and patients under four different recording protocols. The recording protocols are Eyes Open (EO), Eyes Closed (EC), Mental Arithmetic Eyes Open (MAEO) and Mental Arithmetic Eyes Closed (MAEC) conditions. The observed variation of HE in the signals of patients are analysed subsequently.

The average values of HE calculated for all the 23 electrode locations under EC recording protocol for controls and patients are shown in Fig. 3. For all the 23 electrode locations, higher values of HE are observed for patients (Maxim et al. 2005) and the highest value of HE is

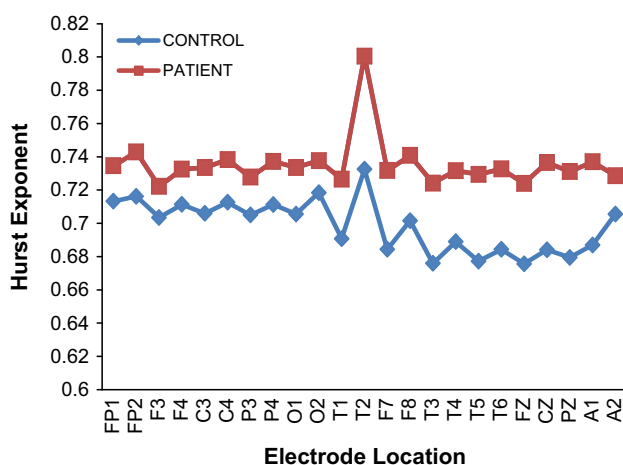


Fig. 3 Values of HE of controls and patients under EC state

observed at the temporal location (T2-recorded from the right half of the brain). The variations in the HE values of the other 22 electrode locations range from 7 to 10% of the value observed at the temporal location T2. A similar trend is observed in the recording protocols under EO, MAEC and MAEO conditions. HE is regarded as a measure of the long-range dependence of a time series, used to determine self-similarity or smoothness of the time series considered. The higher HE values calculated from the EEG signals of Alzheimer patients (MCI-AD) is an indication of the absence of notable irregularity signifying a slowdown of the mental activity of the brain with increase in predictability, long memory, persistent behavior of the signal and low instability of the brain state (Diaz et al. 2015). Though not closely related to the present study, it has been reported that the higher HE value is also an indication that the brain is not able to retain information due to reduction in neuronal oscillations (Montez et al. 2009).

It is now known that any damage to the temporal lobe of a person, by disease or otherwise, ends up with a difficulty in interpreting and memorizing events, leading to the degradation of the ability in organizing and sequencing events and affecting the verbal and visual memory (Bayley et al. 2005; Chan et al. 2001). The early onset of Alzheimer’s disease is also characterized by these attributes in patient’s mental capabilities. The analysis indicates high values of HE at the temporal lobes of the right part of the brain reveals that with the onset of MCI, the particular lobes/regions of the brain gets affected. Considering these facts, one may conclude that the higher values of HE observed in patients is clearly an indication of the early onset of Alzheimer’s.

A comparison of the values of HE for the different lobes (F-Frontal, P-Parietal, O-Occipital and T-Temporal) under various recording protocols of EC, EO, MAEC and MAEO states is carried out and is shown in Fig. 4. It is observed

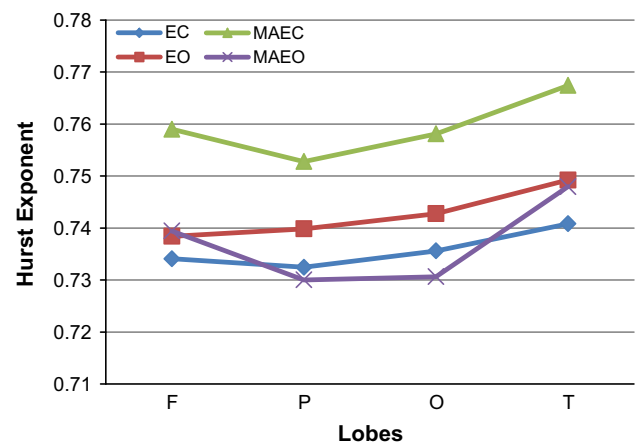


Fig. 4 HE of patients at various lobes under EC, EO, MAEC and MAEO recording protocols

that HE values of patients are the highest for the measurements following MAEC recording protocol. The range of HE values for MAEO and EO protocols are lower from MAEC by 3–4% and 2–3% respectively. Significant group differences were revealed among the different recording protocols of EC, EO, MAEC and MAEO using One-way ANOVA ($F = 8.374$, $df = 3, 88$; $p < 0.000059$) with post hoc Bonferroni alpha corrected p value being 0.00222. Group differences in HE were analysed using a two-way ANOVA with Bonferroni corrections performed in different lobes under different recording protocols. Multiple comparisons using Bonferroni corrections gave a p value of 0.012741 and are found to have high statistically significant difference. The cognitive behavior of the patients under MAEO and EC protocols shows more irregularity in comparison with EO and MAEC states. This clearly indicates that there is a reduction in the chaotic nature of the EEG signal acquired from the MCI-AD patients, thus distinguishing them from normal controls.

The temporal lobe measurements in patients indicate the highest value of HE for all the recording protocols in comparison with the other three lobes (frontal, parietal and occipital). In the recording protocols of EO and EC states, the average HE values are the highest at the temporal followed by occipital, parietal and frontal ($T > O > P > F$). Unlike the EC and EO, MAEC and MAEO recording protocols show higher HE values of 0.75901 and 0.741432 respectively for frontal lobes under mental arithmetic task in comparison to the values observed at occipital and parietal lobes ($T > F > O > P$). The results of HE calculated for different lobes for the MCI-AD patients show that the temporal lobe is affected the most. A notable reduction in the HE values of the signals of the frontal lobe from that of the temporal lobe is observed in MAEC and MAEO protocols. This is in contrast with the observed values of the resting EO and EC states. The value of HE observed in the signals of patients at their frontal lobe indicates that this measure can be related to the decline in the activity of brain. It may be recalled that the frontal lobe is very much involved in problem solving skills, decision making processes and carrying out of various tasks. Impairment in problem-solving and decision making capability of the brain which forms a part of executive functioning has been reported as early manifestations in mild AD patients (Binetti et al. 1996; Chen et al. 2001; Perry and Hodges 1999). The increase in the values in the frontal region is presumed to be a process to sustain the performance of memory during the earlier period of developing AD (Montez et al. 2009). The same is reflected in the present analysis through an observed increase in the HE values of the frontal lobe for MCI-AD patients subjected to mental arithmetic task.

The average value of HE calculated for the lobes under different recording protocols are analysed, for both the left and right hemispheres of the brain and is shown in Fig. 5. Here FL represents Frontal left, FR-Frontal right, P L/R-Parietal left/right, OL/R-Occipital left/right and TL/R-temporal left/right. It is observed that HE values are attenuated in the left hemisphere both under resting state and under task conditions. The increased HE values in the right part of the brain might be due to the reduced complexity and irregularity of the EEG signal which is an indication of the reduction in the processing of information (Lefleche and Albert 1995). Also, this could be an indication of the advancement of the cognitive impairment affecting the right half. It is also inferred from the calculations of HE values that the irregularity of time series is larger in the left half of the brain indicating the possibility of higher impairment in the right half of the brain. It may be noted that the observed trends of higher HE values for the right lobes belong to patients with ($CDR \leq 1$) having an early onset of MCI-AD. The subjects classified under this group are the ones identified to be at an early symptomatic stage of AD representing very mild ($CDR = 0.5$) and mild dementia ($CDR = 1$) (Morris et al. 2001). The severity of cognitive impairment shall differ with an increase in the rating of CDR and there may possibly be a shift in the increase in values of HE from the right hemisphere to the left hemisphere.

The HE values are analyzed at distinct frequency bands of the EEG signal decomposed using db10. Figure 6 shows the six-level Wavelet decomposed EEG signals of control and patients under EC, EO, MAEC and MAEO protocols in the Occipital lobe. Analysis shows that the average values of HE are higher for patients than the controls in all the six levels of Wavelet decomposition. The observed HE values corresponding to the specific frequency band also

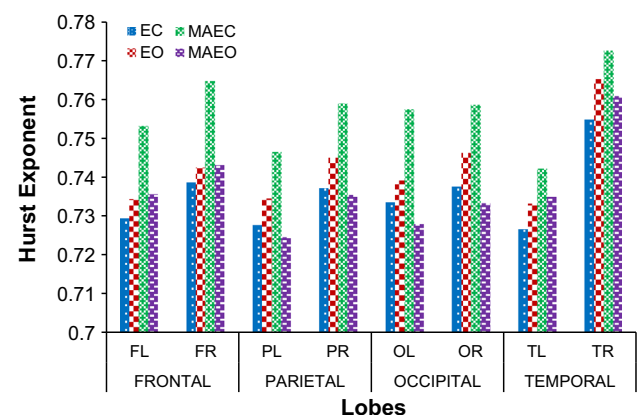


Fig. 5 Comparison of HE at left and right hemispheric lobes of patients under various protocols

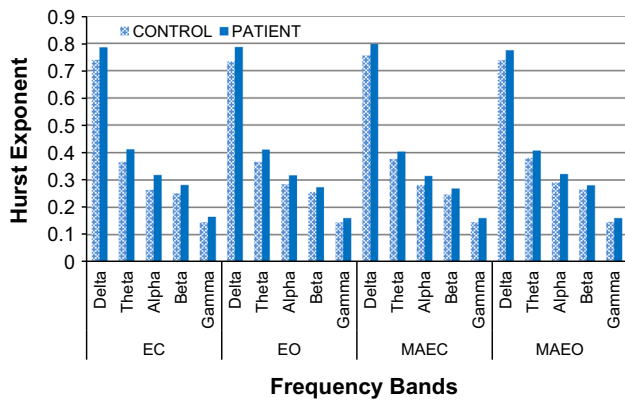


Fig. 6 Comparison of HE values of control and patients for the distinct frequency bands of EEG signal for the Occipital lobe

significantly differ across the brain regions. The nonlinear parameter (HE) calculated for MCI-AD patients shows the highest value in the lower most level of decomposition namely the delta band (0–4 Hz) and the lowest HE value belongs to the higher most level of decomposition namely the gamma band. Amongst the frequency bands, gamma band has more implications in cognitive workload (Diaz et al. 2015) which is very well justified with lower values of HE (Fig. 6). The lower values of HE in gamma band reveal that the functional state of the brain is highly dynamic and unpredictable. The various frequency bands differ by the level of randomness and self-similarity. Higher HE values are observed in patients in the different frequency bands ranging from delta to gamma. High values of HE in delta band show that the system is better ordered, predictable and less complex. The rest of the lobes also give a similar pattern for the values of HE calculated for the different frequency bands under the recording protocols.

Figure 7 shows the comparison of HE at various lobes under the EC protocol. The HE values (shown in Table 3),

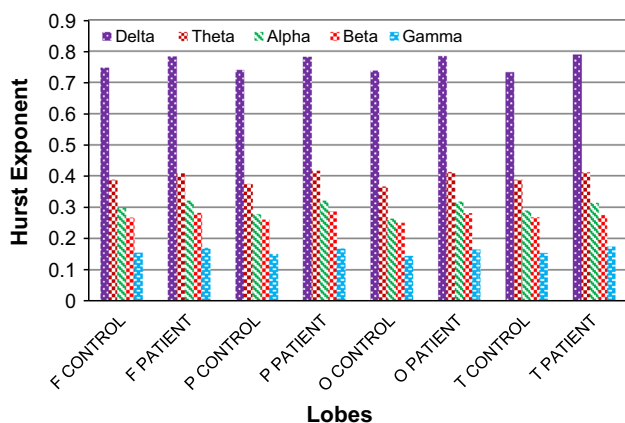


Fig. 7 Comparison of HE values observed at various lobes under EC protocol

Table 3 HE values at different lobes of control and mild AD patients under EC protocol

Lobes	Frequency bands				
	Delta	Theta	Alpha	Beta	Gamma
F Control	0.746522	0.387778	0.29807	0.266309	0.153884
F Patient	0.78248	0.409063	0.32137	0.281388	0.169996
P Control	0.739695	0.374387	0.277623	0.2606	0.150436
P Patient	0.781771	0.415696	0.321264	0.287514	0.167246
O Control	0.73764	0.365535	0.262496	0.249603	0.144396
O Patient	0.784279	0.411943	0.317896	0.280925	0.165025
T Control	0.732459	0.387276	0.288628	0.267505	0.153622
T Patient	0.789101	0.41281	0.314056	0.274776	0.173321

calculated for the various frequency bands indicate that the delta band of the temporal lobe of the mild AD patients record the highest value among all the six levels of decomposition. A similar trend is observed for the remaining three protocols with the smallest value of HE observed in the gamma band for the mild AD patients. This is in conformity with the results shown in Fig. 3. The results of Fig. 7 posit the results in Fig. 6.

In this study, we have also taken effort to verify the correlation between HE, the nonlinear parameter with the age and other neuropsychological indices such as ACE and MMSE scores that are generally used for assessing the severity of AD. Mutual information and bivariate correlation analysis using Pearson’s correlation coefficient and Spearman’s rank correlation coefficient are employed for this purpose.

Spearman correlation coefficients are used to evaluate the associations of HE with age. The statistical independence of HE and age are ensured using One-way ANOVA with the Bonferroni corrected p value being 0.0036571. Table 4 shows the Spearman correlation coefficient of HE with age of controls and patients, calculated specifically for the recording protocols thus integrating the different hemispheres of the brain. A moderate correlation is observed for HE and age using Spearman correlation coefficient ρ , under all the recording protocols for controls and a weak correlation is observed for patients.

Figures 8a, b showst he Pearson correlation between HE with age (in years) of controls and patients respectively. The lobe-vice analysis (shown in Table 5) of Spearman correlation (ρ) of Hurst Exponent with age of patients revealed a low and negative correlation in frontal lobe ($\rho = -0.243, p < 0.0001$) and occipital lobe ($\rho = -0.227, p < 0.001$) with significantly low and negative correlation in temporal ($\rho = -0.189, p < 0.01$) and parietal ($\rho = -0.071, p < 0.005$) for EC recording protocol.

Table 4 Spearman Correlation (ρ) between HE and age of Control and Patient

Subject	EO ($p < 0.05$)	EC ($p < 0.05$)	MAEO ($p < 0.05$)	MAEC ($p < 0.05$)
Control	0.301	- 0.307	0.327	0.349
Patient	- 0.218	- 0.227	0.223	- 0.271

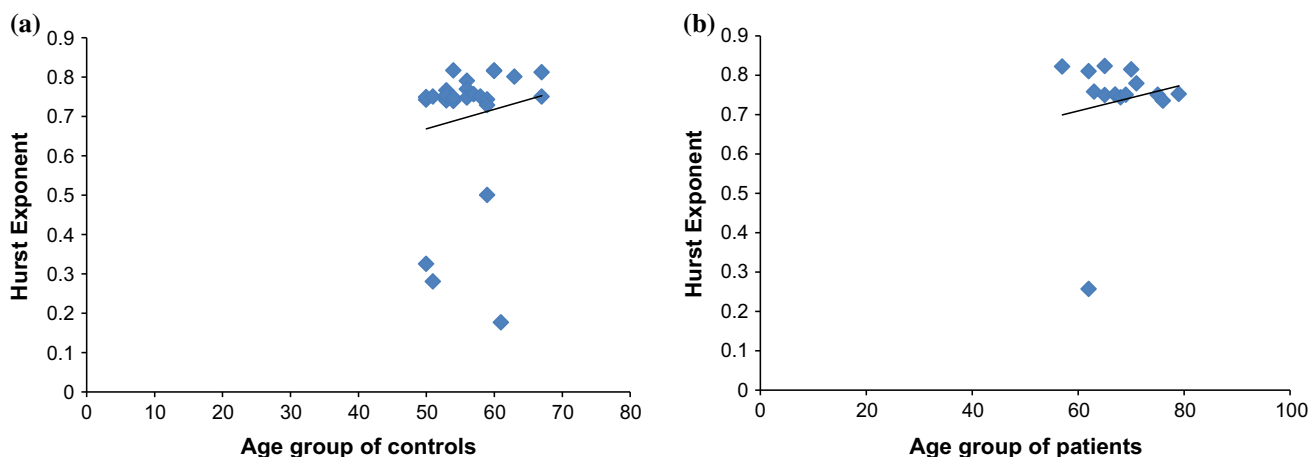


Fig. 8 Correlation between HE and Age under EC protocol of (*Pearson correlation is used for graphical purposes*). **a** Controls ($\rho = 0.1403$, $p < 0.005$) and **b** patients ($\rho = 0.1449$, $p < 0.0001$)

Table 5 Lobe-wise analysis of the Spearman correlation (ρ) of HE with age for patients and controls

Protocols	Lobes							
	Frontal		Parietal		Occipital		Temporal	
	Control	Patient	Control	Patient	Control	Patient	Control	Patient
EC	0.24	- 0.243	0.311	- 0.071	0.276	- 0.227	0.305	- 0.189
EO	0.313	- 0.261	0.302	0.081	0.346	- 0.156	0.357	- 0.183
MAEC	0.334	- 0.21.	0.311	- 0.21	0.357	- 0.21.	0.233	- 0.262
MAEO	0.33	- 0.234	0.185	0.057	0.245	- 0.359	0.25	- 0.225

Similarly, low correlation exists in the frontal ($\rho = -0.261$, $p < 0.02001$) for EO recording protocol with significantly lower correlation in the other three lobes: temporal ($\rho = -0.183$, $p < 0.005$), occipital ($\rho = -0.156$, $p < 0.05$), parietal ($\rho = 0.081$, $p < 0.00005$). For the recording protocol of MAEO, a moderate correlation exists in occipital ($\rho = -0.359$, $p < 0.001$) with significantly low correlations in the frontal ($\rho = -0.234$, $p < 0.05$), temporal ($\rho = -0.225$, $p < 0.0001$) and parietal ($\rho = 0.057$, $p < 0.005$). Similarly, MAEC has low correlation in temporal ($\rho = -0.262$, $p < 0.01$) with significantly low correlations with an average $\rho = -0.21$ ($p < 0.0001$) in the rest of the lobes. For the controls, the temporal ($\rho = 0.305$, $p < 0.001$) and parietal lobe ($\rho = 0.311$, $p < 0.001$) show a moderate correlation under EC recording protocol and a low correlation for the frontal ($\rho = 0.024$, $p < 0.005$) and occipital ($\rho = 0.276$, $p < 0.001$). All the lobes have an average moderate correlation ($\rho = 0.3295$, $p < 0.001$) existing between the age and the HE in EO and MAEC

while the temporal lobe alone have a low correlation ($\rho = 0.233$, $p < 0.001$) in MAEC protocol. In MAEO condition, frontal lobe has a moderate correlation ($\rho = 0.33$, $p < 0.0005$) with the other lobes exhibiting a low correlation with $\rho = 0.226$ ($p < 0.001$).

There exists a negative and moderate correlation only in the occipital region for patients under MAEO recording condition. For the different recording protocols of the controls, the temporal lobe has a moderate correlation under EC and EO recording protocol. The right and left hemispheres of the brain have a moderate correlation existing between age and HE in EO and MAEC protocols except for the temporal lobe in MAEC. Under MAEO protocol, only the frontal lobe has a moderate correlation existing in the controls. Hence it is observed that HE is closely related with age for those moderately correlated values for various lobes in different recording protocols both for patients and controls.

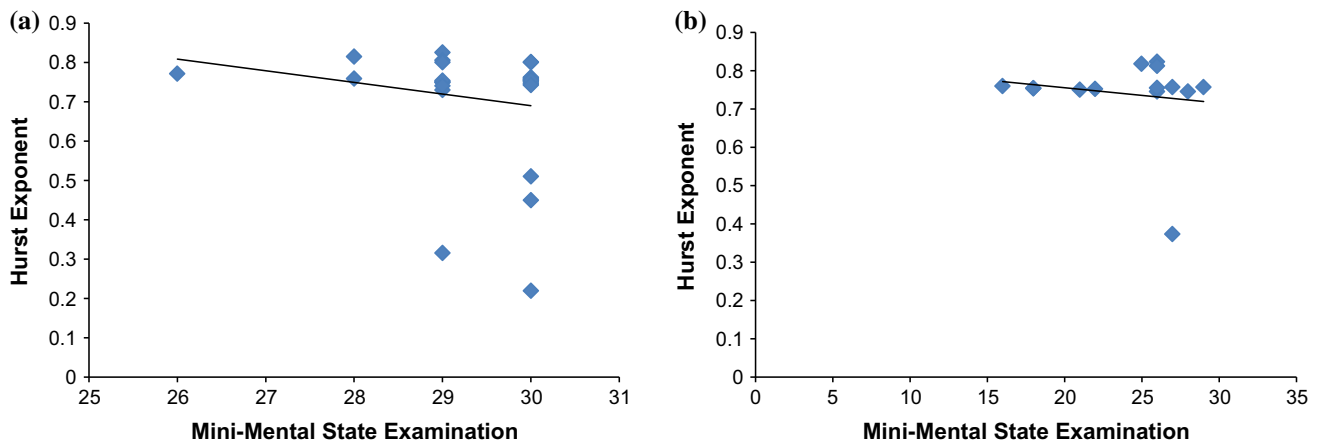


Fig. 9 Scatter plot of HE and MMSE for MAEO protocol of (Pearson correlation is used for graphical purposes). **a** Controls ($\rho = 0.1813$, $p < 0.001$) and **b** patients ($\rho = 0.1514$, $p < 0.001$)

Significant group differences between HE and MMSE are observed using One-way ANOVA with a p -value of 0.0036571 obtained after Bonferroni corrections. Figure 9a, b shows the Pearson correlation between HE and MMSE of controls and patients under MAEO protocol. A moderate Spearman correlation exists in controls between HE and MMSE score in the temporal lobe (average $\rho = 0.328$, $p < 0.001$) for all the recording protocols except for EO ($\rho = -0.181$, $p < 0.0001$) and in the parietal lobe for MAEC ($\rho = -0.36$, $p < 0.001$) and MAEO ($\rho = -0.366$, $p < 0.005$). The rest of the correlation coefficient shows significantly lower values for different lobes under the recording protocols indicating that HE is not closely related with MMSE.

One-way ANOVA with post hoc Bonferroni corrections showed statistically significant difference in group of HE and ACE with a p value of 0.0036571. A negative and moderate Spearman correlation exists in patients between HE and ACE score only in the occipital lobe ($\rho = -0.359$, $p < 0.05$) for MAEO recording protocol. The rest of the lobes and recording protocols have a weak correlation between HE and ACE. A moderate positive correlation exists between HE and Rey Auditory Verbal Learning Test (RAVLT) non-delayed recall score in frontal ($\rho = 0.4$, $p < 0.05$) and temporal ($\rho = 0.307$, $p < 0.05$) for patients in MAEO. The rest of the recording protocols show an average low correlation between HE and RAVLT score ($\rho = 0.232$, $p < 0.05$).

Mutual information analysis

Auto Mutual Information (AMI), similar to entropy measure (Jeong et al. 2001), is calculated for all the recording protocols. The average value of AMI for the controls is in the range of 0.5 to 0.6 whereas the average values for patients lie in the range 0.1 to 0.2. The time delay in the

AMI analysis is 1. Low value of AMI observed in MCI-AD patients is an indication of the reduction in complexity of the brain activity in comparison to the normal controls. The cross mutual information (CMI) helps to assess the dynamic coupling and information transmission between two systems. Here, the average value of CMI employed to calculate the coupling between the HE and age for MCI-AD patients is found to be 3.52 and that for controls is 3.343; between HE and MMSE for patients is 2.8074 and that for controls is 1.4537; between HE and ACE score for patients is 3.3788 and that for controls is 3.6801. The average values of CMIs are larger in patients than in controls except for HE and ACE. The results reveal that there exist a dynamic coupling between HE with age and also HE with MMSE for MCI-AD patients.

The data communication between distinct cortical areas are analysed using mean CMI's calculated over the anterior, posterior and distant brain regions (Jeong et al. 2001; Locatelli et al. 1998). The local anterior CMI is calculated for electrode locations Fp1-F3, Fp1-F7, Fp2-F4 and Fp2-F8 corresponding to the frontal region. Local posterior CMI is calculated for the electrode locations P3-O1, P4-O2, T5-O1 and T6-O2. The distant CMI's are determined between the following electrode pairs: Fp1-P3, Fp1-T5, Fp2-P4, Fp2-T6, P3-F7, P4-F8, F3-P3, F3-T5, F4-P4, F4-T6, F7-T5 and F8-T6. Table 6 represents the mean and standard deviation of the CMI's calculated over the local anterior region, local posterior region and the distant electrode pairs across the central line for the MAEC recording protocol.

Statistical analysis of CMI in MCI-AD patients show prominent decrease in the value in comparison with the normal controls at local anterior, local posterior and distant electrode locations with the lowest value observed in the frontal region. Lower CMI is perceived in AD subjects in local antero-frontal and distant electrodes locations. This establishes the reduction of information transmission in the

Table 6 Mean and standard deviation of CMI's calculated over local anterior, local posterior and distant electrode pairs for normal controls and MCI-AD patients for MAEC protocol

Mean \pm SD	Local anterior electrodes		Local posterior electrodes		Distant electrodes	
	Right	Left	Right	Left	Right	Left
Controls	15.1209 \pm 0.176588	14.98923 \pm 0.055013	15.49772 \pm 0.058431	15.44167 \pm 0.022533	15.27733 \pm 0.144291	15.17976 \pm 0.104627
Patients	13.03479 \pm 0.059949	14.39317 \pm 0.014616	14.59933 \pm 0.015804	15.1759 \pm 0.039669	14.41129 \pm 1.085541	14.97442 \pm 0.439753

corresponding regions of MCI-AD patients in comparison with the healthy subjects. Significantly lower CMI is observed for AD patients in the right hemisphere of the brain, contrary to the observations from the healthy controls.

A lower value of CMI of MCI-AD patients under mental arithmetic state is a direct indication of insufficient data transmission across distinct regions of the brain. Reduction in CMI is a direct indication for the cognitive impairment associated with MCI-AD patients which also supports the fact that there exists impairment in functional activity in the pathways of cortico-cortical fiber in AD subjects as reported by Jeong et al. (2001) and Locatelli et al. (1998).

Discussion

Long range dependence in the EEG signals recorded under four different recording protocols of EC, EO, MAEC and MAEO of MCI-AD and normal controls are analysed using the nonlinear parameter, Hurst exponent. The significance of EEG signal analysis that could reveal the brain dysfunctions in the progression of AD has been widely accepted (Dauwels et al. 2010; Jelles et al. 2008). Simultaneous low pass filtering and total variation denoising (LPF/TVD) algorithm is employed for the EEG signal preprocessing which help in the elimination of both the high and low-frequency noise components (Selesnick et al. 2014). This method of denoising avoids selection and implementation of appropriate transforms. A six-level Multi-resolution decomposition is performed to extract the different EEG signal frequency bands: delta, theta, alpha, beta and gamma, so that the processing will enable us to obtain simultaneous time–frequency information of the signal analysed (Mallat 1989). Adeli et al. (2003) have suggested wavelet transform as an effective tool for investigating discontinuities and periodic patterns of non-linear and non-stationary signals. Discrete Daubechies wavelets are commonly used for Wavelet decomposition. In this study Wavelet-chaos method is used for the analysis of EEG sub-bands and is found to be beneficial for extracting the features of Alzheimer's.

Nonlinear parameters are found to be suitable in the measurement of cortical functions of the brain in AD patients (Jelles et al. 2008). The current study reveals that the average values of HE are higher for MCI-AD patients than the normal controls in all the six levels of wavelet decomposition which is an indication of the slowing down of the electrical activity in patients. Larger values of HE indicates reduced complexity of EEG signal (Vladana 2015). The decrease of EEG complexity might be due to neurotransmitter deficiency and the loss of functional

connectivity due to the death of nerve cell (Gomez et al. 2007; Jelles et al. 1999). The present study shows that the right hemisphere of the brain has much variation in HE for the MCI-AD patients than for the left half. The damage in the right part causes the reduction of nonverbal thinking and also a reason for the inability of motor skills for control (Earle 1988). The lobe wise analysis of HE shows that they are the highest at the temporal lobe. Temporal lobe has a significant role in episodic memory in Alzheimer patients (Ahmadlou et al. 2010). The present results are in agreement with the earlier investigations that the AD progression could be identified with the reduction of irregularity of EEG signal. HE has been widely used in forecasting applications because of its ability to predict the time series (Stan et al. 2014). It is interesting to note that HE is also used for the detection of epileptic seizure (Osorio and Mark 2007) and HE values have shown long range anti-correlation in both epileptic and interictal EEG (Geng et al. 2011). Thus the present study attempts to contribute towards the identification of HE as a meaningful parameter in the detection of AD.

Jelles et al. (2008) reported that the frequency bands of EEG signal signifies distinct brain dynamics. The present study shows that the HE values are the highest in delta band (0–4 Hz) and the lowest in the higher most level of decomposition: Gamma-band (25–50 Hz). Regularity is different for distinct frequency bands of AD because of aberrant neuronal connectivity (Deng et al. 2017). Previous studies have revealed that efficient signal analysis is possible with a combination of Hurst exponent with Wavelet transform (Simonsen et al. 1998).

Age, RAVLT scores and neuropsychological indices such as MMSE, ACE and their relations with Hurst Exponent are verified using Pearson's and Spearman's correlation coefficients. Increased values of correlation coefficients are an indication of correlated time series. Pearson correlation provides linear relations whereas Spearman correlation gives monotonic relations. The lobe wise analysis of correlation coefficients calculated for HE with age, MMSE, ACE and RAVLT scores under various recording protocols differ. The nonlinear parameter of fractal dimension when correlated with age and MMSE are reported to be region dependent (Smits et al. 2016).

Mutual information determines nonrandom relationship between electrode locations. In the present study, Hurst Exponent and Mutual Information analysis are conducted for the quantification of regularity of the AD subjects. Mutual Information technique is usually applied on signals which perceive both linear and nonlinear relationships between time series (Na et al. 2002). Mutual information is reported to be an indicator of cortico-cortical connections in the brain (Min et al. 2003). The present analysis showed reduced values of AMI in MCI-AD which confirms the loss

of coupling between systems and reduction in complexity of the brain activity. Auto mutual information of different electrode locations of patients has lower values in comparison with controls. CMI technique substantiates the quantification of information transmission in the brain. Lower values of CMI observed in local antero-frontal region and distant electrode locations of MCI-AD patients in our study substantiates the reduction in information transmission in these brain regions under mental arithmetic eyes closed state resulting in cognitive decline. Jeong et al. (2001) has reported the lowest CMI in interhemispheric and distant electrode locations when recorded under relaxing eyes open and closed state contrary to our observations. This reduction in information transmission could be due to impairment of cortico-cortical fibers and neuronal death in the brain as reported by Jeong et al. (2001) and Locatelli et al. (1998).

Conclusion

In this study we have investigated the long range dependence in the EEG signals of patients with Alzheimer's having MCI. Hurst Exponent, an index of long range dependence in nonlinear signal analysis, is chosen for the analysis. EEG measurements are carried out on demented and non-demented controls under resting and cognitive task conditions and values of HE are calculated. HE thus obtained is in the range 0.6–1, adopting rescaled τ -range analysis. Here we try to bring in the possible connection with the index of long range dependence with the complexity of the brain activity. Largest HE values are found to be associated with MAEC protocol under which the randomness of the signal is significantly decreased. HE values obtained are higher for MCI-AD patients at the temporal lobe that could be correlated with the patient's observed difficulty in memorizing and interpreting also affecting their visual and verbal memory. HE values are higher in the right hemispherical regions under the resting and cognitive task conditions which could be an indication of the slowing down of their mental activity. HE takes the highest value in the delta EEG frequency band and the lowest in the gamma band for all the recording protocols. This confirms that the mental activity remains higher in the lower frequency bands during the state of disease. Reduced values of auto mutual information and cross mutual information observed in MCI-AD patients is also a clear indication of the reduction of information transmission, relating to the neuronal death and functional impairment in the cortical regions of the brain.

Acknowledgements The authors wish to acknowledge Dr. P.S. Mathuranath for his valuable advice. This research is carried out with

the funding received from Science and Engineering Research Board (DST-SERB- No. SR/FTP/ETA-102/2010), Department of Science and Technology, Government of India.

References

- Abasolo D, Hornero R, Espino P, Poza J, Sánchez CI, de la Rosa R (2005) Analysis of regularity in the EEG background activity of Alzheimer's disease patients with approximate entropy. *Clin Neurophysiol* 116:1826–1834
- Abasolo D, Hornero R, Gómez C, García M, López M (2006) Analysis of EEG background activity in Alzheimer's disease patients with Lempel-Ziv complexity and central tendency measure. *Med Eng Phys* 28:315–322
- Abasolo D, Escudero J, Hornero R, Gómez C, Espino P (2008) Approximate entropy and auto mutual information analysis of the electroencephalogram in Alzheimer's disease patients. *Med Biol Eng Comput* 46:1019–1028
- Abe JM, da Silva LHF, Renato A (2007) Paraconsistent artificial neural networks and Alzheimer disease A preliminary study. *Dement Neuropsychol* 3:241–247
- Adeli H, Zhou Z, Dadmehr N (2003) Analysis of EEG records in an epileptic patient using wavelet transform. *J Neurosci Methods* 123:69–87
- Adler G, Brassen S, Jajcevic A (2003) EEG coherence in Alzheimer's dementia. *J Neural Transm* 110:1051–1058
- Aghajani H, Zahedi E, Jalili M, Keikhosravi A, Vahdat BV (2013) Diagnosis of early Alzheimer's disease based on EEG source localization and a standardized realistic head model. *IEEE J Biomed Health Inform* 17(6):1039–1045
- Ahmadlou M, Hojjat A, Anahita A (2010) New diagnostic EEG markers of the Alzheimer's disease using visibility graph. *J Neural Transm* 117:1099–1109
- Anghinah R, Afonso P, Kanda M, Lopes HF, Fernando L, Basile H et al (2011) Alzheimer's disease qEEG Spectral analysis versus coherence. Which is the best measurement? *Arq Neuropsiquiatr* 69(6):871–874
- Azami H, Daniel A, Samantha S, Javier E (2017) Univariate and multivariate generalized multiscale entropy to characterise EEG signals in Alzheimer's disease. *Entropy* 19(31):1–17
- Babiloni C, Raffaele F, Giuliano B, Andrea C, Gloria DF, Matilde E (2006) Fronto-parietal coupling of brain rhythms in mild cognitive impairment: a multicentric EEG study. *Brain Res Bull* 69:63–73
- Babiloni C, Raffaele F, Giuliano B, Fabrizio V, Giovanni BF, Bartolo L et al (2009) Directionality of EEG synchronization in Alzheimer's disease subjects. *Neurobiol Aging* 30:93–102
- Balli T, Palaniappan R (2010) Classification of biological signals using linear and nonlinear features. *Physiol Meas* 31:1–18
- Bayley PJ, Jeffrey JG, Ramona OH, La Jolla LRS (2005) The neuroanatomy of remote memory. *Neuron* 46:799–810
- Besthorn C, Sattel H, Geiger-Kabisch C, Zerfass R, Förstl H (1995) Parameters of EEG dimensional complexity in Alzheimer's disease. *Electroencephalogr Clin Neurophysiol* 95(2):84–89
- Bhattacharya BS, Cakir Y, Serap-Sengor N, Maguire L, Coyle D (2013) Model-based bifurcation and power spectral analyses of thalamocortical alpha rhythm slowing in Alzheimer's Disease. *Neurocomputing* 115:11–22
- Binetti G, Magni E, Padovani A, Cappa SF, Bianchetti A, Trabucchi M (1996) Executive dysfunction in early Alzheimer's disease. *J Neurol Neurosurg Psychiatry* 60:91–93
- Binnewijzend MAA, Schoonheim MM, Sanz-Arigitia E, Wink AM, van der Flier WM, Tolboom N, Adriaanse SM, Damoiseaux JS, Scheltens P, vanBerckel BNM, Barkhof F (2012) Resting-state fMRI changes in Alzheimer's disease and mild cognitive impairment. *Neurobiol Aging* 33:2018–2028
- Brenner RP, Reynolds CF, Ulrich RF (1988) Diagnostic efficacy of computerized spectral versus visual EEG analysis in elderly normal, demented and depressed subjects. *Electroencephalogr Clin Neurophysiol* 69:110–117
- Breslau J, Starr A, Sicotte N, Higa J, Buchsbaum MS (1989) Topographic EEG changes with normal aging and SDAT. *Electroencephalogr Clin Neurophysiol* 72(4):281–289
- Bron EE, Smits M, Papma JM, Steketee RME, Meijboom R, de Groot M, van Swieten JC, Niessen WJ, Klein S (2017) Multiparametric computer-aided differential diagnosis of Alzheimer's disease and frontotemporal dementia using structural and advanced MRI. *Eur Radiol* 27(8):3372–3382
- Brunovsky M, Matousek M, Edman A, Cervena K, Krajca V (2003) Objective assessment of the degree of dementia by means of EEG. *Neuropsychobiology* 48:19–26
- Buchan RJ, Nagata K, Yokoyama E, Langman P, Yuya H, Hirata Y, Hatazawa J, Kanno I (1997) Regional correlations between the EEG and oxygen metabolism in dementia of Alzheimer's type. *Electroencephalogr Clin Neurophysiol* 103:409–417
- Carlino E, Sigaudo M, Pollo A, Benedetti A, Mongini T, Castagna F, Vighetti S, Rocca P (2012) Nonlinear analysis of electroencephalogram at rest and during cognitive tasks in patients with schizophrenia. *J Psychiatry Neurosci* 37(4):259–266
- Chan D, Fox NC, Scahill RI, Crum WR, Whitwell JL, Leschziner G, Rossor AM, Stevens JM, Cipolotti L, Rossor MN (2001) Patterns of temporal lobe atrophy in semantic dementia and Alzheimer's disease. *Ann Neurol* 49(4):433–442
- Chen P, Ratcliff G, Belle SH, Cauley JA, DeKosky ST, Ganguli M (2001) Patterns of cognitive decline in presymptomatic Alzheimer disease: a prospective community study. *Arch Gen Psychiatry* 58:853–858
- Cichocki A, Shishkin SL, Musha T, Leonowicz Z, Asad T, Kurachi T (2004) EEG filtering based on blind source separation (BSS) for early detection of Alzheimer's disease. *Clin Neurophysiol* 116(3):729–737
- Coben LA, Chi D, Snyder AZ, Storandt M (1990) Replication of a study of frequency analysis of the resting awake EEG in mild probable Alzheimer's disease. *Electroencephalogr Clin Neurophysiol* 75(3):148–154
- Condat L (2013) A direct algorithm for 1D total variation denoising. *IEEE Signal Process Lett* 20(11):1054–1057
- Coronel C, Garn H, Waser M, Deistler M, Benke T, Dal-Bianco P, Ransmayr G, Seiler S, Grossegger D, Schmidt R (2017) Quantitative EEG markers of entropy and auto mutual information in relation to MMSE scores of probable Alzheimer's disease patients. *Entropy* 19(130):1–14
- Cover TM, Thomas JA (1991) Elements of information theory. *J Econ Dyn Control* 20(5):819–824
- Czigler B, Csikós D, Hidasi Z, Gaál ZA, Csibri É, Kiss É, Salacz P, Molnár M (2008) Quantitative EEG in early Alzheimer's disease patients—power spectrum and complexity features. *Int J Psychophysiol* 68:75–80
- Daliri MR (2012) Automated diagnosis of Alzheimer disease using the scale-invariant feature transforms in magnetic resonance images. *J Med Syst* 36:995–1000
- Dauwels J, Vialatte F, Musha T, Cichocki A (2010) A comparative study of synchrony measures for the early diagnosis of Alzheimer's disease based on EEG. *NeuroImage* 49:668–693
- Dauwels J, Srinivasan K, Reddy MR, Musha T, Vialatte FB, Latchoumane C (2011) Slowing and loss of complexity in Alzheimer's EEG: two sides of the same coin? *Int J Alzheimer's Dis* 2011:1–10

- Davatzikos C, Fan Y, Wu X, Shen D, Resnick SM (2008) Detection of prodromal Alzheimer's disease via pattern classification of magnetic resonance imaging. *Neurobiol Aging* 29:514–523
- Davide MV, Babiloni C, Binetti G, Cassetta E, Forno GD, Ferreri F et al (2004) Individual analysis of EEG frequency and band power in mild Alzheimer's disease. *Clin Neurophysiol* 115:299–308
- Deng B, Cai L, Li S, Wang R, Yu H, Chen Y, Wang J (2017) Multivariate multi-scale weighted permutation entropy analysis of EEG complexity for Alzheimer's disease. *Cogn Neurodyn* 11:217–231
- Diaz HM, Córdova FM, Cañete L, Palominos F, Cifuentes F, Sánchez C, Herrera M (2015) Order and chaos in the brain: fractal time series analysis of the EEG activity during a cognitive problem solving task. *Proc Comput Sci* 55:1410–1419
- Dudas RB, Berrios GE, Hodges JR (2005) The Addenbrooke's Cognitive Examination (ACE) in the differential diagnosis of early dementias versus affective disorder. *Am J Geriatr Psychiatry* 13(3):218–226
- Duffy FH, Albert MS, McAnulty G (1984) Brain electrical activity in patients with presenile and senile dementia of the Alzheimer type. *Ann Neurol* 16(4):439–448
- Earle JB (1988) Task difficulty and EEG alpha asymmetry: an amplitude and frequency analysis. *Neuropsychobiology* 20:96–112
- Escudero J, Abásolo D, Hornero R, Espino P, Opez ML (2006) Physiological measurement analysis of electroencephalograms in Alzheimer's disease patients with multiscale entropy. *Physiol Meas* 27:1091–1106
- Fieller EC, Hartley HO, Pearson ES (1957) Tests for rank correlation coefficients. I. *Biometrika* 44(3):470–481
- Folstein MF, Folstein SE, McHugh PR (1975) "Mini-mental state". A practical method for grading the cognitive state of patients for the clinician. *J Psychiatr Res* 12(3):189–198
- Fonseca LC, Maria G, Souza TA, Rodrigues PL, De Amaral AAC (2011) Alzheimer's disease relationship between cognitive aspects and power and coherence EEG measures. *Arq Neuropsiquiatr* 69(6):875–881
- Fonseca LC, Tedrus GMAS, Carvas PN, Machado ECFA (2013) Comparison of quantitative EEG between patients with Alzheimer's disease and those with Parkinson's disease dementia. *Clin Neurophysiol* 124:1970–1974
- Fonseca LC, Tedrus GMAS, Rezende ALR, Giordano HF (2015) Coherence of brain electrical activity: a quality of life indicator in Alzheimer's disease? *Arq Neuropsiquiatr* 73(5):396–401
- Gasser US, Gasser T, Ziegler P (1994) Quantitative EEG analysis in early onset Alzheimer's disease: correlations with severity, clinical characteristics, visual EEG and CCT. *Electroencephalogr Clin Neurophysiol* 90(4):267–272
- Geng S, Zhou W, Yuan Q, Cai D, Zeng Y (2011) EEG non-linear feature extraction using correlation dimension and Hurst exponent. *Neurol Res* 33(9):908–912
- Ghorbanian P, Devilbiss DM, Verma A, Bernstein A, Hess T, Simon AJ, Ashrafiun H (2013) Identification of resting and active state EEG features of Alzheimer's disease using discrete wavelet transform. *Ann Biomed Eng* 41(6):1243–1257
- Ghorbanian P, Devilbiss DM, Hess T, Bernstein A, Simon AJ, Ashrafiun H (2015) Exploration of EEG features of Alzheimer's disease using continuous wavelet transform. *Med Biol Eng Comput* 1–14
- Gomez C, Hornero R, Abásolo D, Fernández Escudero J (2007) Analysis of the magnetoencephalogram background activity in Alzheimer's disease patients with auto-mutual information. *Comput Methods Prog Biomed* 87(3):239–247
- Gordon EB, Sim M (1967) The E.E.G. in presenile dementia. *J Neurol Neurosurg Psychiatr* 30(3):285–291
- Grunwald M, Busse F, Hensel A, Riedel-Heller S, Kruggel F, Arendt T, Wolf H, Gertz HJ (2002) Theta-power differences in patients with mild cognitive impairment under rest condition and during haptic tasks. *Alzheimer Dis Assoc Disord* 16(1):40–48
- Hara J, Shankle WR, Musha T (1999) Cortical atrophy in Alzheimer's disease unmasks electrically silent sulci and lowers EEG dipolarity. *IEEE Trans Biomed Eng* 46(8):905–910
- Hogan MJ, Swanwick GRJ, Kaiser J, Rowan M, Lawlor B (2003) Memory-related EEG power and coherence reductions in mild Alzheimer's disease. *Int J Psychophysiol* 49:147–163
- Hornero R, Escudero J, Fernández A, Poza J, Gómez C (2008) Spectral and nonlinear analyses of MEG background activity in patients with Alzheimer's disease. *IEEE Trans Biomed Eng* 55(6):1658–1665
- Hornero R, Abasolo D, Escudero J, Gómez C C (2009) Nonlinear analysis of electroencephalogram and magnetoencephalogram recordings in patients with Alzheimer's disease. *Phil Trans R Soc A* 367:317–336
- Hughes CP, Berg L, Danziger WL, Coben LA, Martin RL (1982) A new clinical scale for the staging of dementia. *Br J Psychiatry* 140:566–572
- Hurst HE (1951) Long-term storage capacity in reservoirs. *Trans Am Soc Civ Eng* 55:400–410
- Jasper HH (1958) The ten-twenty electrode system of the International Federation. *Electroencephalogr Clin Neurophysiol* 10:371–375
- Jelles B, van Birgelen JH, Slaets JPI, Hekster REM, Jonkman EJ, Stam CK (1999) Decrease of non-linear structure in the EEG of Alzheimer patients compared to healthy controls. *Clin Neurophysiol* 110:1159–1167
- Jelles B, Scheltens Ph, van der Flier WM, Jonkman EJ, Lopes da Silva FH, Stam CJ (2008) Global dynamical analysis of the EEG in Alzheimer's disease: frequency-specific changes of functional interactions. *Clin Neurophysiol* 119:837–841
- Jeong J, Kim SY (1997) Nonlinear Analysis of chaotic dynamics underlying the electroencephalogram in patients with Alzheimer's disease. *J Korean Phys Soc* 30(2):320–327
- Jeong J, Kim SY, Han SH (1998) Non-linear dynamical analysis of the EEG in Alzheimer's disease with optimal embedding dimension. *Electroencephalogr Clin Neurophysiol* 106:220–228
- Jeong J, Gore JC, Peterson BS (2001) Mutual information analysis of the EEG in patients with Alzheimer's disease. *Clin Neurophysiol* 112:827–835
- Jeong DH, Kim YD, Song IU, Chung YA, Jeong J (2016) Wavelet energy and wavelet coherence as EEG biomarkers for the diagnosis of Parkinson's disease-related Dementia and Alzheimer's disease. *Entropy* 18(8):1–17
- Joyce CA, Gorodnitsky IF, Kutas M (2004) Automatic removal of eye movement and blink artifacts from EEG data using blind component separation. *Psychophysiology* 41:1–13
- Kikuchi M, Wada Y, Takeda T, Hiroyasu O, Hashimoto T, Koshino Y (2002) EEG harmonic responses to photic stimulation in normal aging and Alzheimer's disease: differences in interhemispheric coherence. *Clin Neurophysiol* 113:1045–1051
- Kim HT, Kim BY, Park EH, Kim JW, Hwang EW, Han SK, Cho S (2005) Computerized recognition of Alzheimer disease-EEG using genetic algorithms and neural network. *Future Gener Comput Syst* 21:1124–1130
- Klimesch W (1999) EEG alpha and theta oscillations reflect cognitive and memory performance: a review and analysis. *Brain Res Rev* 29:169–195
- Kloppel S, Stonnington CM, Chu C, Draganski B, Schill RI, Rohrer D, Fox NC, Jack CR Jr, Ashburner J, Frackowiak RSJ (2008) Automatic classification of MR scans in Alzheimer's disease. *Brain* 131:681–689

- Koenig T, Prichep L, Dierks T, Hubl D, Wahlund LO, John ER, Jelic V (2005) Decreased EEG synchronization in Alzheimer's disease and mild cognitive impairment. *Neurobiol Aging* 26:165–171
- Labate D, Foresta FL, Morabito G, Palamara I, Morabito FC (2013) Entropic measures of EEG complexity in Alzheimer's disease through a multivariate multiscale approach. *IEEE Sens J* 13(9):3284–3292
- Latchoumane Vincent CF, Ifeachor E, Hudson N, Wimalaratna S, Jeong J (2008) Dynamical nonstationarity analysis of resting EEGs in Alzheimer's disease. *Lect Notes Comput Sci* 4985:921–929
- Lefleche G, Albert MS (1995) Executive function deficits in mild Alzheimer's disease. *Neuropsychology* 9:313–320
- Letemendia F, Pampiglione G (1958) Clinical and electroencephalographic observations in Alzheimer's disease. *J Neurol Neurosurg Psychiatr* 21:167–172
- Leuchter FA, Spar JE, Walter DO, Weiner H (1987) Electroencephalographic spectra and coherence in the diagnosis of Alzheimer's-Type and multi-infarct dementia: a Pilot study. *Arch Gen Psychiatry* 44(11):993–998
- Liu X, Zhang C, Ji Z, Ma Y, Shang X, Zhang Q, Zheng W, Li X, Gao J, Wang R, Wang J, Yu H (2016) Multiple characteristics analysis of Alzheimer's electroencephalogram by power spectral density and Lempel-Ziv complexity. *Cogn Neurodyn* 10:121–133
- Locatelli T, Cursi M, Liberati D, Franceschi M, Comi G (1998) EEG coherence in Alzheimers disease. *Electroencephalogr clin Neurophysiol* 106:229–237
- Loechesa MM, Garcia-Traperoa J, Gilb P, Rubia FJ (1991) Topography of mobility and complexity parameters of the EEG in Alzheimer's disease. *Biol Psychiatr* 30(11):1111–1121
- Mallat SG (1989) A theory for multiresolution signal decomposition: the wavelet representation. *IEEE Trans Pattern Anal Mach Intell* 11(7):674–693
- Mandelbrot B, Wallis JR (1969) Robustness of the rescaled range R/S in the measurement of noncyclic long-run statistical dependence. *Water Resour Res* 5:967–988
- Maxim V, Sendur L, Fadili J, Suckling J, Gould R, Howard R, Bullmore E (2005) Fractional Gaussian noise, functional MRI and Alzheimer's disease. *Neuroimage* 25:141–158
- McKhann G, Drachman D, Folstein M, Katzman R, Price D, Stadlan EM (1984) Clinical diagnosis of Alzheimer's disease: report of the NINCDS-ADRDA Work Group under the auspices of Department of Health and Human Services Task Force on Alzheimer's disease. *Neurology* 34:939–944
- Melissant C, Ypma A, Frietman EEE, Stam CJ (2005) A method for detection of Alzheimer's disease using ICA-enhanced EEG measurements. *Artif Intell Med* 33:209–222
- Min BC, Jin SH, Kang IH, Lee DH, Kang JK, Lee ST, Sakamoto K (2003) Analysis of mutual information content for EEG responses to odor stimulation for subjects classified by occupation. *Chem Senses* 28:741–749
- Mishra P, Singla SK (2013) Artifact Removal from biosignal using fixed point ICA algorithm for pre-processing in biometric recognition. *Meas Sci Rev* 13(1):7–11
- Mizuno T, Takahashi T, Cho RY, Kikuchi M, Murata T, Takahashi K, Wada Y (2010) Assessment of EEG dynamical complexity in Alzheimer's disease using multiscale entropy. *Clin Neurophysiol* 121(9):1438–1446
- Montez T, Poil SS, Jones BF, Manshanden I, Verbunt JPA, van Dijk BW, Brussaard AB, van Ooyen A et al (2009) Altered temporal correlations in parietal alpha and prefrontal theta oscillations in early-stage Alzheimer disease. *PNAS* 106(5):1614–1619
- Morabito FC, Labate D, Foresta FL, Bramanti A, Morabito G, Palamara I (2012) Multivariate multi-scale permutation entropy for complexity analysis of Alzheimer's disease EEG. *Entropy* 14:1186–1202
- Morabito FC, Labate D, Bramanti A, Foresta FL, Morabito G, Palamara I, Szu HH (2013) Enhanced compressibility of EEG signal in Alzheimer's disease patients. *IEEE Sens J* 13(9):3255–3261
- Morris JC, Storandt M, Miller JP, McKeel DW, Price JL, Rubin EH, Berg L (2001) mild cognitive impairment represents early-stage Alzheimer disease. *Arch Neurol* 58:397–405
- Na SH, Jin SH, Kim SY, Ham BJ (2002) EEG in schizophrenic patients: mutual information analysis. *Clin Neurophysiol* 113:1954–1960
- Nasrolahzadeh M, Mohammadpoory Z, Haddadnia J (2016) A novel method for early diagnosis of Alzheimer's disease based on higher-order spectral estimation of spontaneous speech signals. *Cogn Neurodyn* 10(6):495–503
- Nuwer M (1997) Assessment of digital EEG, quantitative EEG, and EEG brain mapping. *Neurology* 49:277–292
- Osorio I, Mark GF (2007) Hurst parameter estimation for epileptic seizure detection. *Commun Inf Syst* 7(2):167–176
- Park YM, Che HJ, Im CH, Jung HT, Bae SM, Lee SH (2008) Decreased EEG synchronization and its correlation with symptom severity in Alzheimer's disease. *Neurosci Res* 62:112–117
- Perry RJ, Hodges JR (1999) Attention and executive deficits in Alzheimer's disease. A critical review. *Brain* 122:383–404
- Petit D, Lorrain D, Gauthier S, Montplaisir J (1993) Regional spectral analysis of the REM sleep EEG in mild to moderate Alzheimer's disease. *Neurobiol Aging* 14(2):141–145
- Pijnenburg YAL, vd Made Y, van Cappellen van Walsum AM, Knol DL, Scheltens Ph, Stam CJ (2004) EEG synchronization likelihood in mild cognitive impairment and Alzheimer's disease during a working memory task. *Clin Neurophysiol* 115:1332–1339
- Podgorelec V (2012) Analyzing EEG signals with machine learning for diagnosing Alzheimer's disease. *Elektronika Ir Elektrotehnika* 18(8):61–64
- Pogarell O, Teipel SJ, Juckel G, Gootjes L, Möller T, Bürger K, Leinsinger G, Möller H-J, Hegerl U, Hampel H (2005) EEG coherence reflects regional corpus callosum area in Alzheimer's disease. *J Neurol Neurosurg Psychiatry* 76:109–111
- Prinz PN, Vitiell MV (1989) Dominant occipital (alpha) rhythm frequency in early stage Alzheimer's disease and depression. *Electroencephalogr Clin Neurophysiol* 73(5):427–432
- Pu J, Xu H, Wang Y, Cui H, Hu Y (2016) Combined nonlinear metrics to evaluate spontaneous EEG recordings from chronic spinal cord injury in a rat model: a pilot study. *Cogn Neurodyn* 10(5):367–373
- Pucci E, Cacchio G, Angeloni R, Belardinelli N, Nolfè G, Signorino M, Angeleri F (1998) EEG spectral analysis in Alzheimer's disease and different degenerative dementias. *Arch Gerontol Geriatr* 26:283–297
- Pucci E, Belardinelli N, Cacchio G, Signorino M, Angeleri F (1999) EEG power spectrum differences in early and late onset forms of Alzheimer's disease. *Clin Neurophysiol* 110:621–631
- Rae GA, Blume W, Lau C, Hachinski VC, Fisman M, Merskey H (1987) The electroencephalogram in alzheimer-type dementia: a sequential study correlating the electroencephalogram with psychometric and quantitative pathologic data. *Arch Neurol* 44(1):50–54
- Raghavan N, Glover JR, Sheer DE (1986) A microprocessor-based system for diagnosis of cognitive dysfunction. *IEEE Trans Biomed Eng* 33(10):942–948
- Rosenberg SJ, Ryan JJ, Prifitera A (1984) Rey auditory-verbal learning test performance of patients with and without memory impairment. *J Clin Psychol* 40(3):785–787

- Rudin LI, Osher S, Fatemi E (1992) Nonlinear total variation based noise removal algorithms. *Physica D* 60:259–268
- Sankari Z, Adeli H, Adeli A (2011) Intra-hemispheric, inter-hemispheric, and distal EEG coherence in Alzheimer's disease. *Clin Neurophysiol* 122:897–906
- Selesnick IW, Graber HL, Pfeil DS, Barbour RL (2014) Simultaneous low-pass filtering and total variation denoising. *IEEE Trans Signal Process* 62(5):1109–1124
- Simonsen I, Hansen A, Nes OM (1998) Determination of the Hurst exponent by use of wavelet transforms. *Phys Rev E* 58(3):2779–2787
- Smits FM, Porcaro C, Cottone C, Cancelli A, Rossini PM, Tecchio F (2016) electroencephalographic fractal dimension in healthy ageing and Alzheimer's disease. *PLoS ONE* 11(2):1–16
- Snaedal J, Johannesson GH, Gudmundsson TE, Gudmundsson S, Pajdak TH, Johnsen K (2010) The use of EEG in Alzheimer's disease, with and without scopolamine—a pilot study. *Clin Neurophysiol* 121:836–841
- Snaedal J, Johannesson GH, Gudmundsson TE, Blin NP, Emilsdottir AL, Bjorn E, Johnsen K (2012) diagnostic accuracy of statistical pattern recognition of electroencephalogram registration in evaluation of cognitive impairment and dementia. *Dement Geriatr Cogn Disord* 34:51–60
- Sperling RA, Bates JF, Chua EF, Cocchiarella AJ, Rentz DM, Rosen BR, Schacter DL, Albert MS (2003) fMRI studies of associative encoding in young and elderly controls and mild Alzheimer's disease. *Neurol Neurosurg Psychiatry* 74:44–50
- Stam CJ, Montez T, Jones BF, Rombouts SAR, van der Made Y, Pijnenburg YAL, Scheltens Ph (2005) Disturbed fluctuations of resting state EEG synchronization in Alzheimer's disease. *Clin Neurophysiol* 116:708–715
- Stam CJ, de Haan W, Daffertshofer A, Jones BF, Manshanden I, van Cappellen van Walsum AM et al (2009) Graph theoretical analysis of magnetoencephalographic functional connectivity in Alzheimer's disease. *Brain* 132:213–224
- Stan C, Cristescu CM, Cristescu CP (2014) Computation of hurst exponent of time series using delayed (Log-) returns. Application to estimating the financial volatility. *U.P.B. Sci Bull Ser A* 76(3):235–244
- Stigsby B, Jóhannesson G, Ingvar DH (1981) Regional EEG analysis and regional cerebral blood flow in Alzheimer's and Pick's diseases. *Electroencephalogr Clin Neurophysiol* 51(5):537–547
- Stoub TR, Bulgakova M, Leurgans S, Bennett DA, Fleischman D, Turner D, deToledo-Morrell L (2005) MRI predictors of risk of incident Alzheimer disease A longitudinal study. *Neurology* 64(9):1520–1524
- Tóth B, File B, Boha R, Kardos Z, Hidasi Z, Gaál ZA, Csibri É, Salacz P, Stam CJ, Molnár M (2014) EEG network connectivity changes in mild cognitive impairment—Preliminary results. *Int J Psychophysiol* 92:1–7
- Tsai PH, Lin C, Tsao J, Lin PF, Wang PC, Huang NE, Lo MT (2012) Empirical mode decomposition based detrended sample entropy in electroencephalography for Alzheimer's disease. *J Neurosci Methods* 210:230–237
- Vladana (2015) Automated nonlinear analysis of newborn electroencephalographic signals. Doctoral Thesis 1:100
- Vorobyov S, Cichocki A (2002) Blind noise reduction for multisensory signals using ICA and subspace filtering, with application to EEG analysis. *Biol Cybern* 86:293–303
- Wada Y, Yuko N, Jiang ZY, Koshino Y, Yamaguchi N, Hashimoto T (1997) Electroencephalographic abnormalities in patients with presenile dementia of the Alzheimer type: quantitative analysis at rest and during photic stimulation. *Biol Psychiatry* 41:217–225
- Wan B, Ming D, Qi H, Xue Z, Yin Y, Zhou Z, Cheng L (2008) Linear and nonlinear quantitative EEG analysis. *IEEE Eng Med Biol Mag* 27:58–63
- Wang K, Liang M, Wang L, Tian L, Zhang X, Li K, Jiang T (2007) Altered functional connectivity in early Alzheimer's disease: a resting-state fMRI study. *Hum Brain Mapp* 28:967–978
- Wang R, Wang J, Yu H, Wei X, Yang C, Deng B (2015) Power spectral density and coherence analysis of Alzheimer's EEG. *Cogn Neurodyn* 9:291–304
- Waser M, Deistler M, Garn H, Benke T, Dal-Bianco P, Ransmayr G (2013) EEG in the diagnostics of Alzheimer's disease. *Stat Papers* 54:1095–1107
- Waser M, Garn H, Schmidt R, Benke T, Dal-Bianco P, Ransmayr G, Schmidt H (2016) Quantifying synchrony patterns in the EEG of Alzheimer's patients with linear and non-linear connectivity markers. *J Neural Transm* 123:297–316
- Woyshville MJ, Calabrese JR (1994) Quantification of occipital EEG changes in Alzheimer's disease utilizing a new metric: the fractal dimension. *Biol Psychiat* 35(6):381–387
- Yang AC, Wang SJ, Lai KL, Tsai CF, Yang CH, Hwang JP, Lo MT, Huang NE, Peng CK, Fuh JL (2013) Cognitive and neuropsychiatric correlates of EEG dynamic complexity in patients with Alzheimer's disease. *Prog Neuropsychopharmacol Biol Psychiatry* 47:52–61
- Yi GS, Wang J, Deng B, Wei XL (2017) Complexity of resting-state EEG activity in the patients with early-stage Parkinson's disease. *Cogn Neurodyn* 11(2):147–160
- Yuvaraj R, Murugappan M (2016) Hemispheric asymmetry non-linear analysis of EEG during emotional responses from idiopathic Parkinson's disease patients. *Cogn Neurodyn* 10(3):225–234